How to Engineer Organic Solvent Resistant Enzymes: Insights from Combined Molecular Dynamics and Directed Evolution Study

Haiyang Cui,[a] Tom H. J. Stadtmüller,[a] Qianjia Jiang,[a] Karl-Erich Jaeger,[b] Ulrich Schwaneberg,*[a, c] and Mehdi D. Davari*[a]

Expanding synthetic capabilities to routinely employ enzymes in organic solvents (OSs) is a dream for protein engineers and synthetic chemists. Despite significant advances in the field of protein engineering, general and transferable design principles to improve the OS resistance of enzymes are poorly understood. Herein, we report a combined computational and directed evolution study of *Bacillus subtlis* lipase A (BSLA) in three OSs (i.e., 1,4-dioxane, dimethyl sulfoxide, 2,2,2-trifluoroethanol) to devise a rational strategy to guide engineering OS resistant enzymes. Molecular dynamics simulations showed that OSs reduce BSLA activity and resistance in OSs by (i) stripping off essential water molecules from the BLSA surface mainly through H-bonds binding; and (ii) penetrating the substrate binding cleft leading to inhibition and conformational change. Interestingly, integration of computational results with "BSLA-SSM" variant library (3439 variants; all natural diversity with amino acid exchange) revealed two complementary rational design strategies: (i) surface charge engineering, and (ii) substrate binding cleft engineering. These strategies are most likely applicable to stabilize other lipases and enzymes and assist experimentalists to design organic solvent resistant enzymes with reduced time and screening effort in lab experiments.

1. Introduction

Biocatalysts are widely applied in chemical and pharmaceutical industries.[1] Numerous industrially relevant enzymatic reactions have been proposed and optimized for use in organic (co-) solvents (OSs). Improvements comprise increased activity and stability, increased solubility of hydrophobic substrates/products, ease of product recovery, ability to shift the thermodynamic equilibrium toward new reactions, and others.[2] Moreover, the use of OS-water reaction medium also provides opportunities for the enzymatic production of synthetic targets with poor water solubility.[2b,3] Enzymatic reactions conducted in OSs have the great industrial potential[4] since they would enable to combine the synthetic power of enzymes with chemical synthesis efficiently. However, the vast majority of enzymes show reduced or no catalytic activity in OSs.[5]

Several studies of enzymes in OSs have reported effects of OSs on enzymatic structure and function,[2a,6] which are pieces in a complex puzzle. Molecular dynamics (MD) simulations have complemented experimental data and provided some molecular insights into the negative effects of OSs on enzymes.[7] Increased understanding of the interaction and molecular changes in enzyme structure and catalytic mechanism in OSs has promoted the development of many complementary methods, such as stabilizing additives and protein engineering strategies, to stabilize enzymes and increase resistance of enzymes in OSs.[8] It is generally accepted that the interactions between enzymes and OSs mostly depend on the molecular structure and properties of OSs.[3,8] The effect of OSs on enzymes have mainly been reflected in five aspects: (a) conformational changes within enzyme,[3,9] (b) loss of enzyme bound water that is crucial for activity,[10] (c) competitive inhibition by OS molecules,[11] (d) solubility change of the substrate,[10d] and (e) stabilization of the charged transition state.[12] Compared with non-polar solvents, polar OSs can often penetrate deeper into enzymes, and therefore are more capable of inducing destructive secondary and tertiary structural changes. In addition, polar solvents can easily strip off essential water molecules, which affects protein structure and function.[10b–d] Interestingly, water activity (a_w), an indicative of water content around enzymes, significantly affects catalytic activity of lipase in OS.[10a,11b,13] Studies have shown that the

[a] H. Cui, T. H. J. Stadtmüller, Q. Jiang, Prof. U. Schwaneberg, Dr. M. D. Davari
Lehrstuhl für Biotechnologie
RWTH Aachen University
Worringerweg 3
52074 Aachen (Germany)
E-mail: u.schwaneberg@biotec.rwth-aachen.de
m.davari@biotec.rwth-aachen.de
[b] Prof. K.-E. Jaeger
Institute of Molecular Enzyme Technology
Heinrich Heine University
Düsseldorf and Research Center Jülich
Wilhelm Johnen Strasse
52426 Jülich (Germany)
[c] Prof. U. Schwaneberg
DWI-Leibniz Institute for Interactive Materials
Forckenbeckstraße 50
52074 Aachen (Germany)

Supporting information for this article is available on the WWW under https://doi.org/10.1002/cctc.202000422

effect of OSs on enzyme stability and flexibility also depends on the "type" of enzyme.[3,9] MD studies of *Candida antarctica* lipase B (CALB) in tert-butyl alcohol, methanol, methyl tert-butyl ether, and hexane cosolvents show that residence times of OS decreased with increased a_w which is usually accompanied with higher enzyme flexibility.[14] With regard to structural integrity, enzymes are much more tolerant of non-polar OSs than polar ones. Kamal and co-workers[15] demonstrated that methanol and isopropanol made the structure of *Bacillus subtlis* lipase A (BSLA) less rigid and more prone to unfolding, which led to increased instability of BSLA. The reported pieces of the puzzle on role of OSs on enzymes indicate a need for further studies to solve the OSs puzzle. A comprehensive understanding of such interactions is especially important for protein engineers to design OS resistant enzymes.

Directed evolution has matured into a powerful approach to improve enzymes for the production of chemicals and pharmaceuticals as documented by the Nobel Prize in Chemistry in 2018.[16] Several studies in which amino acid positions for improvement in OSs were identified through directed evolutions campaigns have been reported.[17] For instance, it was reported that the hydrogen bonds formed by polar or charged amino acids in loop regions are crucial to retaining enzyme stability in a hydrophilic OS.[17a] Interestingly, it was found that the evolved variant DhaA80, carrying four hydrophobic/polar substitutions in the access tunnel of haloalkane dehalogenase DhaA, doubled its resistance to polar OS dimethyl sulfoxide (DMSO).[17g] Furthermore, CALB and BSLA beneficial substitutions toward OS resistance were preferred to be surface-exposed.[17a,c] In summary, directed evolution has proven to be a powerful method to discover different pieces of the puzzle on how to stabilize enzymes in OSs. However, since traditional directed evolution campaigns have been reported to find less than 20% of the beneficial positions,[17c] the obtained datasets are insufficient to obtain a full picture on interactions that stabilize enzymes in OSs.

Site Saturation Mutagenesis (SSM)-libraries of a whole gene, which contain the full natural diversity at each amino acid position, are an effective strategy to obtain a full picture on the stability landscape and provide detailed insight into sequence-function relationships.[18] Exploring the effects of all interactions possibilities offered by nature is likely a prerequisite to discover general design principles[19] and thereby solve the enzyme-OSs interaction puzzle. Such an SSM library has been reported for BSLA in our previous work, termed as "BSLA-SSM" library (181 positions, in total 3440 variants).[18f,20] The "BSLA-SSM" library screened towards improved resistance in three OSs (22% (v/v) 1,4-dioxane (DOX), 60% (v/v) DMSO, 12% (v/v) 2,2,2-trifluoroethanol (TFE)).[20–21] DOX, DMSO, TFE were chosen since they are among the most common organic media for enzymatic catalysis.[17c,22] Besides, the three OSs and OSs-water mixtures are often chosen for use as a cryoprotective agent, internal standard or in studies involving the (un)folding of proteins, membrane permeability, or chemical synthesis.[23]

Herein, we used an integrative approach by combining computational studies based on the analysis of the "BSLA-SSM" library with experimental results to deeply understand interactions of BSLA with the OSs (DOX; DMSO; TFE) at molecular level. Based on our analysis, we proposed two complementary rational strategies to guide protein engineering efforts towards improved OSs resistance.

2. Results

The molecular dynamics (MD) simulations and directed evolution results on BSLA are presented in four parts to generate a comprehensive understanding of OSs effect on the BSLA. Firstly, we studied the solvation of the BSLA by water/OSs through analysis of structural and dynamic properties, e.g., spatial distribution function (SDF), hydration shell, OS solvation level, radial distribution function (RDF), and solvent contact frequency. Secondly, the "BSLA-SSM" experimental library was analyzed to support the computational observation by identifying amino acid substitutions patterns on the BLSA surface. In the third part, analysis of specific interactions in substrate binding cleft, leading to inhibition of BSLA by OSs, was investigated through local solvation analysis and kinetics experiments. Subsequently, the patterns of resistant/non-resistant amino acid substitutions in the substrate binding cleft were investigated in detail.

2.1. BSLA solvation in organic cosolvents

We analyzed the influence of three cosolvents (DOX, DMSO, TFE) on the overall structure and flexibility of BSLA (see details in SI, Figure S1–S10). The overall structure of BSLA remains stable in DOX, DMSO and TFE throughout the 100 ns simulation. The results demonstrated that the overall conformational change of BSLA is not the predominant reason for BSLA activity and resistance reduction in OSs. In order to understand the effects of OSs on the hydration of the BSLA, the distribution of water and OSs molecules at the BSLA surface were examined with SDF of water and OSs (Figure 1). Analysis of BSLA in water shows that some waters interact closely with the BSLA surface and form water networks (Figure 1a). A comparison between the BSLA in water (Figure 1a) and OSs (Figure 1b-d) shows that water molecules are stripped off by the OS molecules, and the OS molecules penetrate crevices, causing a heterogeneous distribution of OSs at the BSLA surface. The OS distribution at the BSLA surface was localized in certain regions, only leaving other regions of the BSLA surface in contact with water. The removal of water molecules from the BSLA surface is more evident in the substrate binding cleft for all three OSs, especially for DMSO and TFE, which might result in reducing catalytic activity because of the competition with the substrate (see Section 2.3).

The hydration shell and OSs solvation level were quantified to shed further light on the role of water and OS molecules' behavior. As shown in Table 1, the hydrogen level decreases compared to water following the trend DOX > DMSO > TFE. As indicated, the number of water molecules around BSLA in all three OSs was remarkably reduced compared to in water only

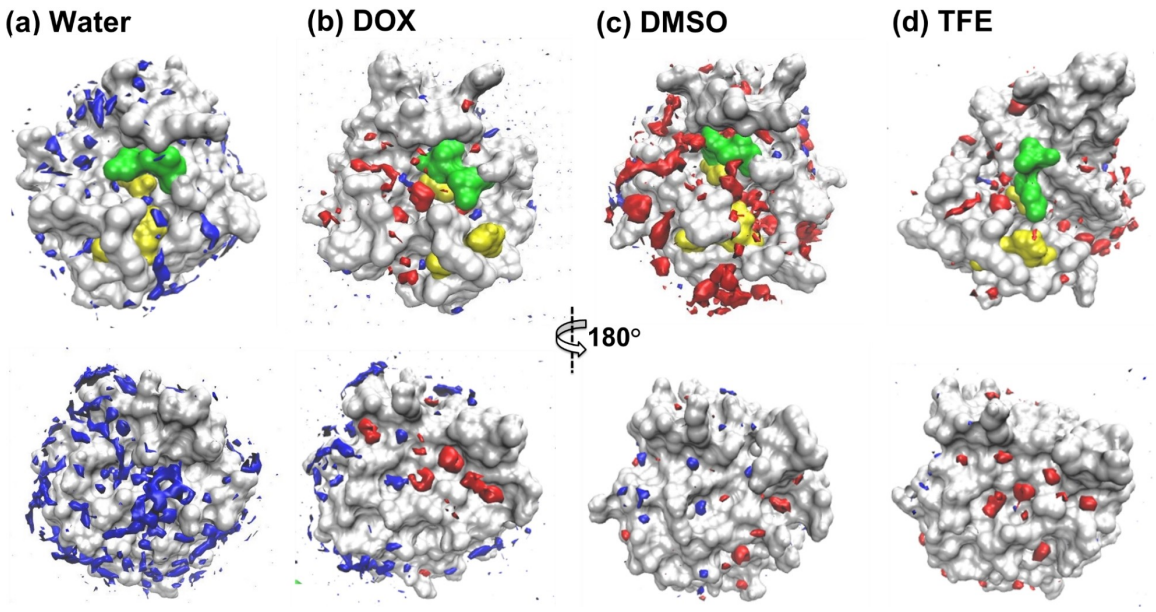

Figure 1. Spatial distribution of water and OS molecules at the molecular surface of the BSLA in (a) Water, (b) DOX, (c) DMSO, and (d) TFE cosolvents averaged over the last 40 ns of MD simulations. The BSLA surface is shown in grey, Ser77, Asp133, His156 (the catalytic triad) in yellow, and Ile12, Met78 (oxyanion hole) in green; the OS molecules in red, the water molecules in blue. For each solvent, two sides of BSLA are shown in order to give a complete view of the surface. Each view of BSLA has the same orientation in all solvents. The contours are shown with the isovalue 8.5 for water, and isovalue 50, 13, 54 for DOX, DMSO, TFE molecules, respectively.

Table 1. Hydration level and OS solvation level of BSLA in water and different OSs during MD simulations.

Solvent	Hydration level[a]	OS solvation level[b]
Water	373.7 ± 3.6	–
DOX	261.6 ± 5.8	122.5 ± 5.8
DMSO	204.2 ± 4.9	2305.0 ± 55.5
TFE	190.7 ± 10.0	213.8 ± 8.3

[a] Hydration level averaged over the last 40 ns of MD trajectories. Water molecules whose O atom is within 3.5 Å distance cutoff of any non-hydrogen atom of BSLA were described as the first hydration shell and the number of water as hydration level[14]. A similar definition was also applied to OS solvation level, [b] OS solvation level averaged over the last 40 ns of trajectories. The cut-off distance was determined from the radial distribution function (RDF) of OSs around BSLA residues when the "central" atom of OS molecule showed first minima approximately at this distance[14]. The "central" atom for DMSO, TFE is S2, C2, respectively (see Figure 2b, c). Since DOX does not have the "central" atom, we applied the average cut-off of the atoms at two para positions (C1 and C3, Figure 2a). Consequently, a 6.8 Å cut-off was employed for DOX, DMSO, and TFE.

system, which indicated that water molecules were vigorously stripped off from the BSLA surface by OSs. In contrast to hydrogen level trend, OS solvation level decreases in the following order: DMSO > TFE > DOX. The results correlate well with the qualitative picture from SDF analysis of OS or water molecules on the BSLA (Figure 1b–d).

In order to determine the driving force for stripping off the water molecules by OSs, we investigated the orientation of surrounding solvent molecules by calculating the radial distribution function (RDF) of OSs relative to the BSLA surface (Figure 2). The RDFs suggested that the oxygen group of DOX is closer to the BSLA surface than the carbon backbone (Figure 2a), the oxygen group of DMSO is closer than the methyl group (Figure 2b), and the hydroxyl group of TFE is closer than the fluorine group (Figure 2c). Overall, OS molecules tended to accumulate near the surface of the BSLA with a similar orientation, in which the oxygen atom preferred to orient towards the BSLA surface. A similar orientation showed the possibility to form H-bond with BSLA, indicating that the H-bond interaction could be the dominant interaction in this case. However, the oxygen atom of OSs can play different roles when it forms the H-bond with amino acids on the BSLA surface, e.g., as H-acceptor in the case of DOX, DMSO and as H-donor in TFE.

In order to identify the OS's preferred amino acid type for interaction with the BSLA surface, the time-averaged surface residue-water/OS contact frequencies were calculated. The minimum distance of < 2.5 Å was chosen as the cutoff of residue-water/OS contact to identify the strong interactions.[24] As shown in Figure 3 and Figure S11 in SI, all types of surface residues show relatively high contact frequency (66–99%) with water molecules in water system with the following trend: non-polar (66%) < polar (86%) < negatively charged (99.8%) ≈ positively charged (99.9%). Latter indicates that positively and negatively surface charged amino acids preferred to attract more water molecules when compared with polar and non-polar amino acids. The OSs contact frequency results are shown in Figure 3. Although the OSs showed very different trends, however, the OSs mainly compete with water molecules for polar and negatively charged residues on the BSLA surface. Also, the different trends towards water and OSs could provide the hint that stabilizing the enzyme could be possible through the introduction of one specific type of amino acid with relatively higher water attraction but lower OS interaction.

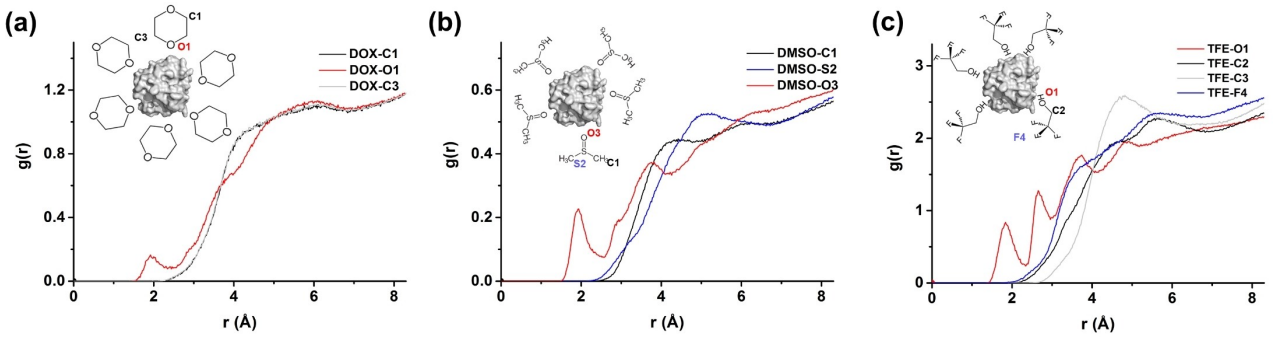

Figure 2. The orientation of OSs on the BSLA surface: (a) For DOX, the RDFs were calculated for the DOX oxygen atom (O1) and two para carbons (C1, C3) around the BSLA residues, respectively. (b) For DMSO, the RDFs were calculated for the DMSO carbon atom (C1), sulfur atom (S2), and oxygen atom (O3) around the BSLA residue, respectively. (c) For TFE, the RDFs were calculated for the TFE oxygen atom (O1), two carbon atoms (C2, C3), fluorine atom (S2), and around the BSLA residues, respectively. Figures inset show the chemical structure for OSs and BSLA in each cosolvent.

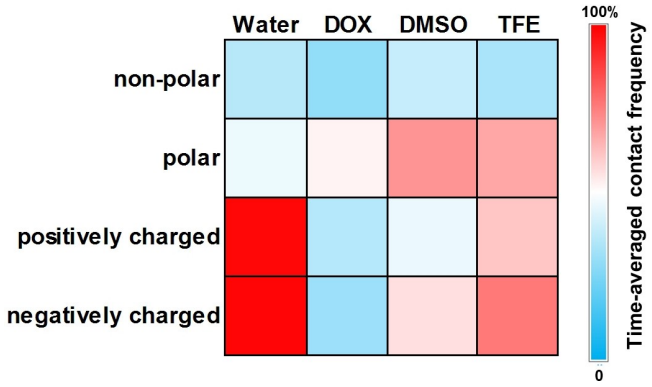

Figure 3. Time-averaged frequency of contacts between the BSLA surface amino acids and water/DOX/DMSO/TFE molecule in water, DOX solvents, DMSO solvents, TFE solvents, respectively. The following amino acid classification was used: Non-polar: G, A, V, L, I, M, F, W, P. Polar: S, T, C, Y, N, Q. Negatively charged: D, E. Positively charged: K, R, H. Contact frequency was defined as the average percentage of different surface residue-OS molecule contacts in the last 40 ns of three independent MD simulation runs. Residue-OS contact was defined as residue-water/OS molecule distance being 2.5 Å or less. The total number of frames in the last 40 ns of three MD runs were normalized to 100%.

Among four types of amino acids, positively charged one seemed to be the most promising selection, this hypothesis was indeed confirmed by the "BSLA-SSM" library experiment (see Section 2.2).

2.2. Analysis of amino acid substitutions on the BSLA surface from "BSLA-SSM" library

The results from MD simulations presented in Section 2.1 showed that OSs interact mainly with BSLA surface residues. In order to associate the MD results to directed evolution experiments, we reanalyzed all the beneficial substitutions (DOX: 159 substitutions; DMSO: 371; TFE: 181) and beneficial positions (DOX: 75 positions; DMSO: 107; TFE: 74) from "BSLA-SSM" library (in total 181 positions; 3439 variants).[17c] As a general trend shown in Table S1 and Figure S12–14 in SI, surface-exposed substitutions (54–73%) were more preferred to improve all three selected OSs resistance than buried substitutions (27–46%), indicating surface residues play an essential role in tolerating OSs. Among all the beneficial positions, mostly (41–51%) positions were exchanged by charged substitutions. Surprisingly, 91–94% beneficial positions, which harboring charged substitutions, were substituted from uncharged amino acids to charged amino acids (see Figure 4, DOX: 92% (35/38); DMSO: 91% (39/43); TFE: 94% (30/32)). Furthermore, analysis of amino acid classifications of beneficial substitutions on BSLA surface shows that positively charged substitutions predominantly (36–53%) improved OS resistance compared to others, as shown in Table 2.

Significantly improved substitutions are usually applied to perform the trend of how to engineer enzymes in directed evolution. In "BSLA-SSM" library, there were in total 12, 18, and 38 substitutions with high resistance (>2-fold resistance improvement compared to BSLA wild type) towards DOX, DMSO, and TFE, respectively (Table S2–S4). Among them, 34–42% (DOX: 5 substitutions; DMSO: 8; TFE: 13) were exchanged by charged amino acid. Besides, positively charged substitutions were also more prominent when compared to others. Consequently, by analyzing beneficial and top resistant substitutions (>2-fold resistance improvement), we confirmed that surface positively charged substitutions were preferred to

Table 2. Analysis of amino acid classification of surface beneficial substitutions from "BSLA-SSM" library[a].

Organic cosolvent	Non-polar [%](variant)	Polar [%] (variant)	Negatively charged [%](variant)	Positively charged [%] (variant)
DOX	17% (47)	16% (35)	14% (8)	53% (48)
DMSO	20% (110)	16% (68)	25% (28)	39% (69)
TFE	18% (54)	19% (46)	27% (17)	36% (35)

[a] All percentage values are normalized to BSLA amino acid composition, as BSLA amino acid composition is not evenly distributed (43% non-polar, 34% polar, 9% negatively charged, and 14% positive charged amino acid). The following amino acid classification was used: Non-polar: G, A, V, L, I, M, F, W, P. Polar: S, T, C, Y, N, Q. Negatively charged: D, E. Positively charged: K, R, H.

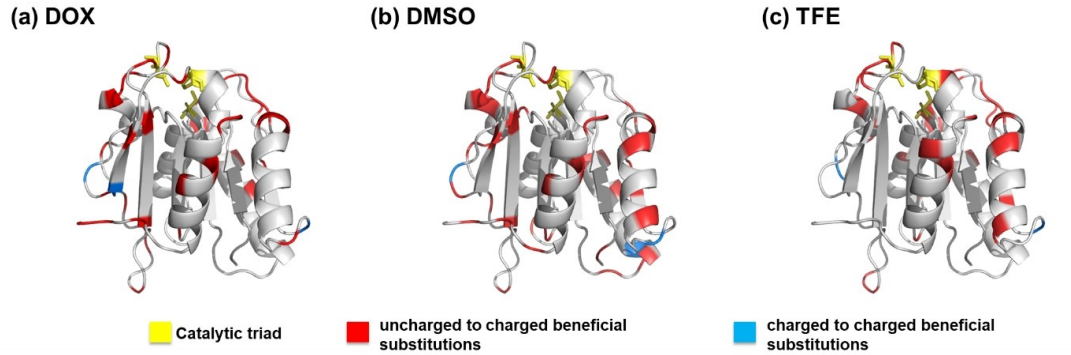

Figure 4. BSLA beneficial positions (charged amino acid substitutions) for improvement of resistance in (a) DOX, (b) DMSO, and (c) TFE. The BSLA structure is shown as cartoon in grey, the catalytic triad (Ser77, Asp133, and His156) is shown as stick in yellow, amino acid positions of uncharged to charged beneficial substitutions are shown in red, amino acid positions of charged to charged beneficial substitutions are shown in blue.

improve the OSs resistance, which points in the same direction with the observation in Section 1.

2.3. Analysis of the BSLA substrate binding cleft

The substrate binding cleft of the BSLA is solvent-exposed since it lacks the lid present in other lipases. According to RMSF analysis (Figure S2a), the highest local flexibility was observed in OSs simulation for the region around L8 and α4 (amino acid 151–165), especially in TFE. The observed relatively high RMSF for the α4 helix was interesting as one of the catalytic triads (His156: $RMSF_{Water} = 0.77 \pm 0.02$ Å, $RMSF_{DOX} = 1.42 \pm 0.28$ Å, $RMSF_{DMSO} = 1.61 \pm 0.28$ Å, $RMSF_{TFE} = 2.4 \pm 0.24$ Å) is located in this region. However, three OSs did not show a significant effect on the flexibility of the other two catalytic residues (Ser77 and Asp133). Additionally, SASA analysis revealed that Ser77 and His156 are more exposed in all three OSs (Figure S15 in SI). Hence, OSs render the side chains of in the substrate binding cleft more mobile, which further confirmed by the distance analysis between the catalytic triad residues in the following section.

In the BSLA crystal structure, the distance between Asp133-OD1 and His156-ND1 is 2.7 Å that suggests a strong H-bond between Asp133 and His156.[25] Another strong H-bond was formed between Ser77-OG and His156-NE2 (2.8 Å) in the substrate binding cleft. The distance between Asp133-OD1 and His156-ND1 did not show significant change during the MD simulations in water and OSs (Figure 5b). However, the catalytically relevant H-bond between Ser77-OG and His156-NE2 was broken because of Ser77-OG···His156-NE2 distance significantly increased from ~4.5 Å (in water) to 6–12 Å in OSs (Figure 5a). Interestingly, two Ser77-OG···His156-NE2 distance distribution peaks were appeared in TFE, indicating that the substrate binding cleft might have two populated conformations. This observation was also correlated to oxyanion hole configuration change in TFE in which Ile12-N···Met78-N distance had two distance distribution peaks, as shown in Figure 5c. Furthermore, compared with water, the increased distance in OSs indicated that the configuration of substrate binding cleft changes in OSs. In contrast, the distance between the oxyanion hole residues (Ile12-N···Met78-N) was decreased, which might influence the stabilization of the negatively charged reaction intermediates[25] or even change the substrate specificity.[26]

The SDF (Figure 1) shows that the density of each OS is relatively high near the substrate binding cleft, which indicates an apparent affinity of the solvent molecules for the substrate binding site. In order to examine how the water or OS molecule behaves in the substrate binding cleft of BSLA, the average number of water (N_{water}) and OS (N_{OS}) in the BSLA substrate binding cleft were calculated based on the last 40 ns of the MD trajectories, and the results are shown in Figure 6 and Table 3. We defined the BSLA substrate binding cleft as the region (Figure 5d), which expands 5.9 Å away from the Ser77 residue located at the bottom of the BSLA substrate binding cleft. As shown in Table 3, BSLA substrate binding cleft was well hydrated with ~8 water molecules in water. Interestingly, about two water molecules remained in the BSLA substrate binding cleft in DOX. One water molecule (WATER1, Figure 6a) formed an H-bond with Ser77-O and was preserved in substrate binding cleft (Figure S16 in SI). One DOX molecule (DOX2) was hydrated through bifunctional H-bonds with WATER1[28] and retained in the substrate binding cleft. As shown in Figure 6b and Figure S17 in SI, another DOX molecule (DOX1) always bridged between His156 and Ser77 in substrate binding cleft, indicating DOX molecule can directly disturb proton transfer from Ser77 to His156 in acylation steps (Figure 5a and Figure 6a). All the water molecules were stripped off from the substrate binding cleft and replaced by two DMSO molecules in

Table 3. The average number of solvent molecules (OSs or water) in BSLA substrate binding cleft during the MD simulations in water and OSs[a].

Solvent	N_{water}	N_{OS}
Water	7.9 ± 2.8	
DOX	2.2 ± 0.8	2.8 ± 0.8
DMSO	0	2.1 ± 0.7
TFE	0	1.1 ± 0.5

[a] The number of water and OS molecules, averaged over the last 40 ns from three independent MD runs, denotated as N_{water} and N_{OS}, respectively.

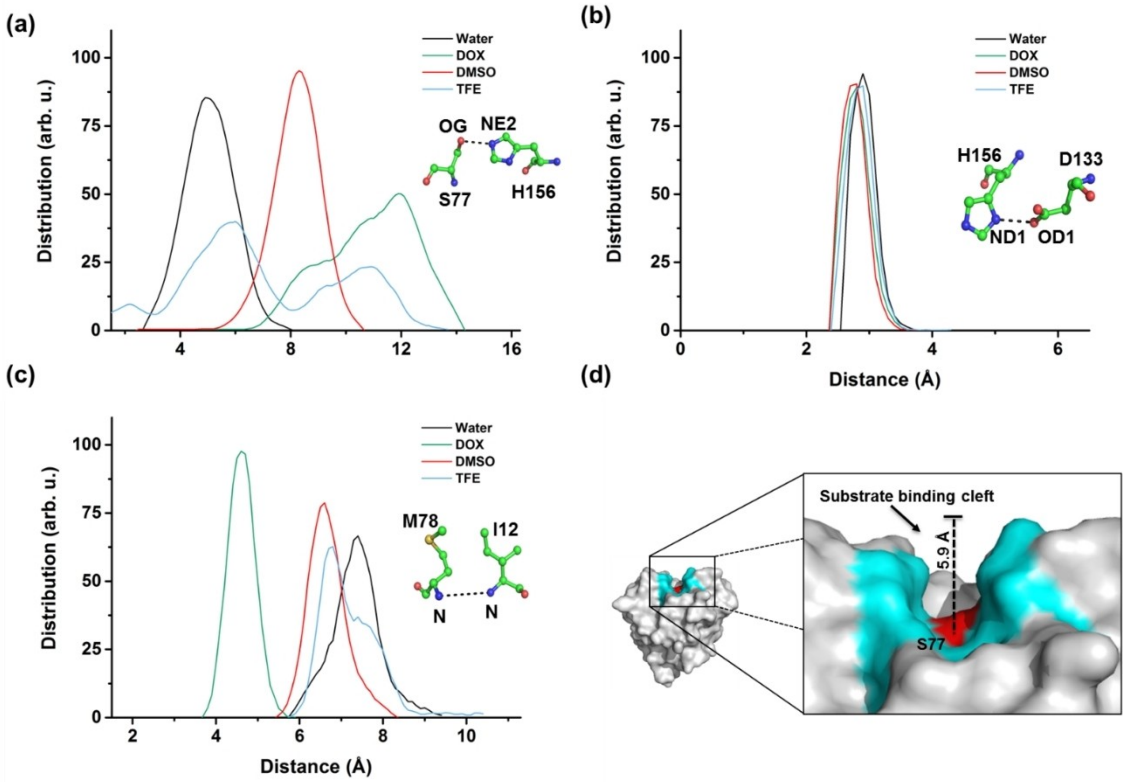

Figure 5. Interatomic distance distributions curve between the catalytic triad (Ser77, His156, Asp133) and oxyanion hole (Ile12, Met78) of BSLA in water (black), DOX (green), DMSO (red) and TFE (blue): (a) Ser77-OG···His156-NE2 (b) His156-ND1···Asp133-OD1 and (c) Ile12-N···Met78-N. Representative structures of the catalytic triad and oxyanion hole were selected based on cluster analysis of the MD trajectories. The catalytic triad and oxyanion hole are shown as ball-and-stick with carbon (green), oxygen (red), nitrogen (blue). The dashed line indicates the distance between two atoms. (d) A close-up view from substrate binding cleft of BSLA. The BSLA surface is shown in grey, substrate binding cleft of BSLA in cyan, Ser77 (part of the catalytic triad) in red. The depth of Ser77 residue from BSLA surface was calculated by Depth server [27].

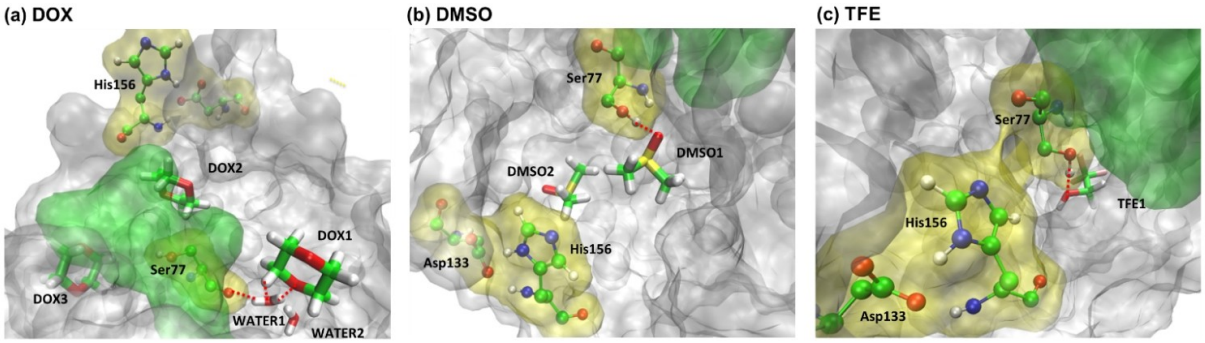

Figure 6. Solvation of the BSLA substrate binding cleft in (a) DOX, (b) DMSO, and (c) TFE, respectively. Representative structures of the substrate binding and solvent molecules were selected from the last 40 ns of MD trajectories. The BSLA surface is shown in grey, catalytic triad (Ser77, Asp133, and His156) in yellow, oxyanion hole (Ile12, Met78) in green. The catalytic triad is also shown as ball-and-stick with carbon (green), oxygen (red), nitrogen (blue), hydrogen (white). OS and water molecules are shown as sticks with carbon (green), oxygen (red), hydrogen (white), sulfur (yellow), fluorine (pink). The dashed line (red) indicates an H-bond between two atoms.

DMSO cosolvent (Figure 6b and Table 3). Besides, one H-bond was formed between Ser77-OG and DMSO1-O3 (Figure 6b and Figure S18), which might lead to inhibition of nucleophilic attacking from Ser77 in acylation steps. A similar observation found in TFE cosolvent but with only one TFE molecule in substrate binding cleft (Figure 6c). Although TFE has both H-acceptor and H-donor character, TFE-O1 forms H-bond with Ser77-OG, indicating H-donor capability plays a primary role in reducing the BSLA activity (Figure S19). These results indicated that H-bond interactions between catalytic triad (especially Ser77) and OS molecules mainly lead to the inhibition and BSLA activity reduction. Additionally, a detailed analysis of interaction

energy, including the binding energies ($\triangle G_{binding}$), the van der Waals ($\triangle E_{vdW}$), and electrostatic energy ($\triangle E_{elec}$), between catalytic triad/oxyanion hole and OS molecules agrees well with the above solvation phenomenon (see details in SI, Figure S20a–c).

To experimentally confirm the inhibition behavior by OSs, characterization studies of the purified BSLA in water and the selected OSs were carried out with pNPB activity assay. The obtained K_m and k_{cat} for BSLA in Table 4 closely match with reported values.[29] The BSLA in all three OSs showed decreased turnovers (k_{cat}) and profitless effects on the pNPB substrate recognition (increased K_m values). Overall, DOX, DMSO, TFE decreased the catalytic efficiency (k_{cat}/K_m) to 45.3%, 34.5%, 48% compared with the BSLA in water, respectively. The above results confirmed the potent inhibition of three OSs towards the BSLA.

2.4. Analysis of amino acid substitutions in BSLA substrate binding cleft from "BSLA-SSM" library

Generally, the substitutions in the BSLA substrate binding cleft are directly correlated to the inherent function of the enzyme. From the catalytic mechanism of lipase, it is believed that substrate binding is typically one of the rate-limiting steps preceding catalytic reaction.[18c,30] Therefore, we performed molecular docking based on the substrate pNPB to identify the most critical residues in the substrate binding cleft. Molecular docking studies (Figure S21) revealed that apart from the catalytic triad residues (Ser77, Asp133, and His156), the seven non-polar (hydrophobic) residues (Ile12, Met78, Ala105, Leu108, Ile135, Val136, Leu140) were also involved in the interaction with the pNPB. Figure S22 in SI summarizes the OSs resistance of the identified substrate binding positions from the "BSLA-SSM" experimental library. After screening of the SSM libraries of seven non-polar amino acids positions (in total 134 substitutions = 7 positions × 19 substitutions + wild type), 14 (10%), 21 (16%), and 20 (15%) beneficial substitutions were obtained for DOX, DMSO, and TFE resistance, receptively. These beneficial substitutions were located on mostly (57–71%) identified substrate-contacting positions. The preferred amino acid type to improve resistance in the substrate binding cleft was non-polar (≈42.9%) for all three OSs (Table 5). Interestingly, non-polar substitutions also showed the lowest fatality rate (7.8–18.9%, Table 5). This agrees with the evolutionary conservation analysis of amino acid residues that the seven substrate-contacting residues were not well conserved but mainly exchanged by non-polar residues (Figure S23 and Table S5 in SI). These results suggested that the proper hydrophobicity of substrate binding cleft would contribute to the binding of the hydrophobic substrates.[31]

Subsequently, we investigated both residue-OS contact frequency and substrate (pNPB) binding affinity (by molecular docking) to reveal the potential molecular mechanism for beneficial non-polar variants located in substrate binding cleft (Figure S24 in SI and Table S6). The seven identified substrate-contacting non-polar residues, on average, did not show high contact frequency compared to the polar and charged catalytic triad (Figure S24 in SI), which agrees well with the overall trend for the whole BSLA (Figure 3). Among beneficial non-polar substitutions (in total, 6–9), three common non-polar substitutions (I12 A, I12 W, L140 A) showed improved resistance towards all three OSs. Five common non-polar substitutions (I12 V, I12 M, M78G, V136 L, L140G) showed improved resistance towards two OSs. Besides, not surprisingly, the highly exposed catalytic triad residues Ser77, Asp133, and His156 show high contact frequency with all three OSs, especially His156 (His156-DOX: 81%; His156-DMSO: 90%; His156-TFE: 73%, Figure S24 in SI). This high contact frequency might lead to the relatively high flexibility of His156 located in α4 helix (See Figure S2c). Generally, binding affinity from the molecular docking using substrate in catalytically competent docking poses can be correlated with catalytic efficiency of enzyme.[32] The docking results of eight BSLA variants and wild type are described in Table S6. Notably, all beneficial non-polar variants showed an increased absolute value of binding energy compared to BSLA wild type, indicating the substrate pNPB has a higher binding affinity to the beneficial non-polar substitutions. In summary, the low contact possibility of OS and high

Table 4. Kinetic characterization of the purified BSLA in water and OSs. The pNPB assay was used to measure kinetic characterization[a].

Solvent	K_m [mM]	k_{cat} [min^{-1}]	k_{cat}/K_m [mM^{-1} min^{-1}]
Water	0.51 ± 0.02	185 ± 4	362
DOX	0.57 ± 0.03	93 ± 5	164
DMSO	0.65 ± 0.03	81 ± 4	125
TFE	0.78 ± 0.02	136 ± 6	174

Table 5. [a] Kinetic parameters were determined by fitting the calculated reaction rates to the Michaelis-Menten equation using software Origin pro 8.6.Table 5
Classification of beneficial and inactive amino acid substitutions in BSLA substrate binding cleft[a].

	Organic solvent	Amino acid type [%] (variant number)			
		Non-polar	Polar	Positively charged	Negatively charged
Beneficial rate	DOX	42.9% (6)	42.8% (6)	14.3% (2)	0.0% (0)
	DMSO	42.9% (9)	33.3% (7)	9.5% (2)	14.3% (3)
	TFE	42.9% (8)	28.6% (6)	19.0% (4)	9.5% (2)
Fatality rate	DOX	17.7% (16)	26.6% (24)	36.6% (33)	50.0% (45)
	DMSO	7.8% (6)	13.3% (11)	19.9% (16)	45.0% (37)
	TFE	18.9% (17)	26.6% (23)	30.0% (26)	45.0% (40)

[a] The positions were identified from molecular docking, and the catalytic triad positions were excluded during the calculation. Beneficial rate is defined as the number of all beneficial substitutions divides the number of one type beneficial substitutions. Similar definition is for fatality rate.

substrate affinity are two dominant reasons for non-polar amino acids in substrate binding cleft to improve OS resistance.

3. Discussion

Routinely employing enzymes in OSs enable exciting possibilities in biocatalysis for chemical production. Numerous enzyme classes (e.g., hydrolases,[7a,11a,33] oxidoreductases,[34] transferases,[8] transpeptidase[35]) have been successfully tailored toward improved OS resistance by using protein engineering methods. By integrating results from computational studies with "BSLA-SSM" experimental library data, this study provided molecular insight into the effect of OSs on BSLA. These findings were used in turn to devise general rational protein engineering strategies to improve the resistance of lipase in OSs.

3.1. Organic solvents strip off essential waters from the BSLA surface

Enzymes generally require some essential water molecules bound to the surface of enzymes to maintain protein structure, dynamics, and function.[4c,36] The addition of water molecules can increase both the kinetics and flexibility of enzymes in OSs.[37] Although water activity (a_w) is an important experimental factor for enzyme activity in non-aqueous media (e.g., pure OSs),[5a] however, it is challenging to predict critical hydration level in polar OSs.[38] MD simulations can provide fundamental insight into the role of solvation at the molecular level. The SDF, hydration shell and/or OS layer results of all three OSs (DOX, DMSO and TFE) for BSLA agree well with the prevailing view that polar OS molecules can disturb the hydration shell of the enzyme surface.[22,39] As we observed from OS orientation and contact frequency analysis (Figure 3 and Figure 4), H-bond interaction is most likely the primary interaction between BSLA and OSs when compared to hydrophobic interactions and van der Waals interactions. On the BSLA surface, all groups capable of forming H-bonds, especially polar amino acid side chains, are most likely form H-bond to OS molecules (e.g., the H-bond acceptor: DOX, DMSO; H-bond acceptor/donor: TFE). The similar phenomenon about DMSO interaction was reported by Afonso and coworkers,[22] that polar amino acid side chains of peptide sMTM7 have dipole-dipole interactions with the oxygen atom of DMSO and form H-bond. Compared to hydrophilic OSs (e.g., DMSO, TFE, acetonitrile), hydrophobic OSs (e.g., hexane, methyl tertiary butyl ether) possess less ability to remove the essential water from the enzyme surface because of missing active H-bond acceptor/donor.[3,40] Overall, solvation data for BSLA in OSs suggested that H-bond interaction with the BSLA surface might be the critical factor for competing with essential water molecules on the BSLA surface, which leads to the destruction of hydration shell. Undoubtedly, the functions (e.g., activity, stability, resistance) of BSLA would be influenced by losing essential water molecules from the BSLA surface.

3.2. Inhibition and conformational change of active site reduce the BSLA activity

Polar OSs usually show an apparent affinity towards the active site and act as an inhibitor to enzymes (e.g., lipase,[11] subtilisin,[41] cellulase[42]). The kinetic experiments in combination with solvation behavior studies of substrate binding cleft (see Section 2.3) strongly supported inhibition as one of the explanations for activity reduction of the BSLA in the OSs. Also, as the overall solvation of the whole BSLA showed, H-bond interaction also has a crucial role in the solvation of the substrate binding cleft (Figure 6). Generally, different solvent molecules have different binding affinity towards active site of enzymes,[11a] indicating that inhibition behavior is related to not only the OS but also to the enzyme. For instance, Roccatano and coworkers found that DMSO molecules were not able to diffuse into the substrate binding site of cytochrome P450 BM-3 during the 15 ns of simulation.[43] The H-bond interaction between OSs-amino acid residues indicates that inhibition behavior might be the main reason for the change of the structure and flexibility substrate binding cleft region (see Figure 5 and Figure S2c). In previous studies, similar behavior was found for *Candida rugose* lipase (CRL) that CCl4 rendered the side chains in the hydrophobic substrate binding site of CRL more mobile.[44] These results also confirmed that local protein dynamics are associated with solvents interaction.[37,45] Thereby, except inhibition and water stripping off, the conformational change caused by the interaction of OSs with residues in the substrate binding cleft could also be another main factor that influences the enzyme activity.[46]

3.3. General principles to stabilize lipase in OSs

By a combination of computational results and the "BSLA-SSM" library dataset, two complementary rational strategies to improve BSLA resistance in OSs are proposed:

(i) Surface charge engineering (introduction of positively charged residues)
By analyzing the BSLA-solvent interaction in MD simulation and beneficial substitutions pattern in "BSLA-SSM" library, we confirmed that the surface positively charged substitutions is the best candidate to improve the OS resistance (see Section 2.1 and 2.2). The possible mechanism is explained as follow: introduction of surface positively charged residues could attract more water molecules to prevent interaction with OSs, which result in stronger hydration shell and weaker OS layer. To render lipases stable in OSs, the surface property and surface charge distribution of lipases are usually the dominant deciding factors.[33a] These finding encourage us to propose the surface charge engineering strategy, which can be applied to the overall protein surface. The proposed surface charged engineering strategy matches well with generally accepted concept that positively charged residue plays important roles in keeping functional protein structure (e.g., favoring solubilization of protein and peptide in water,[47]

modifying the orientation and configuration of multi-subunit complex,[48] and even affecting membrane binding[49]). This strategy also agrees well with the report that most lipases having equivalent surface-exposed positive and negative charged residues were stable in a wide range of OSs.[33a] A newly introduced, surface-exposed charge either form a new salt bridge, build an isolated charge, or break a preexisting salt bridge. However, our previous comprehensive structural analysis of "BSLA-SSM" library illustrated that the formation of salt bridges by newly introduced charged residues is of minor importance for increased resistance to water-miscible OSs.[17c] The newly introduced "isolated" charged amino acid might mainly contribute to stabilize the enzyme and increase the OSs resistance by synergically attracting the water molecules and breaking the OSs layer. In terms of the potential application, surface charge engineering could be applied for engineering not only the stability of enzymes in non-conventional media (e.g., OSs,[17c,50] ionic liquids,[19,51] detergents), but also other enzyme properties (e.g., pH-activity,[52] oxidative stability[53]).

(ii) Substrate binding cleft engineering (introduction of non-polar residues)

How to ingeniously tailor the amino acids in the substrate binding cleft is always a challenge for protein engineers. According to the pattern of substitutions and molecular understanding in Section 2.3 and 2.4, we found non-polar substitutions in substrate binding cleft would be in favor of improving the stability of BSLA in OSs. The beneficial non-polar substitutions in substrate binding cleft most likely prevent OSs access to the active sites and increase substrate binding affinity, which would significantly decrease the inhibition phenomenon caused by OSs. Although substitutions close to the active site might reduce enzyme activity to some extent, however, it is still possible to improve the OS resistance (i.e., lipase activity in OS/its activity in buffer) and activity in parallel.[54] The non-polar substrate binding cleft engineering strategy could be implemented with CASTing,[55] CompassR[56] and focused mutagenesis method with reduced amino acid alphabet[57] to design smart libraries with minimum experimental effort. For reducing the OSs interaction or tailoring the binding affinity, the introduction of a single substitution might not be enough to retain the enzyme activity. Numerous reports point out that further improved variants could be obtained by recombining beneficial substitutions.[58] Hence, combined strategies could be implemented with multi-site mutagenesis methods (e.g., ISM,[59] Iterative CASTing,[55a] OmniChange,[60] PTRec[61] and StEP[62]) to guide recombination of beneficial substitutions identified from directed evolution campaigns, and thereby speed up the design of significantly improved OSs resistant enzymes.

4. Conclusion

In summary, the integrative computational studies and directed evolution experiments ("BSLA-SSM" library) discovered that: i) three predominant factors (stripping off water, flexibility and conformational change of the substrate binding cleft, and solvent inhibition) impair BSLA activity; ii) H-bonds interactions of BSLA and water/OS have a primary influence on the BSLA structure, solvation behavior, and activity; iii) surface charge engineering (introduction of positively charged substitutions) and substrate binding cleft (introduction of non-polar substitutions) engineering strategies could serve as general rational protein engineering principles to stabilize lipases in OSs and might apply to other enzymes sharing a similar α/β-hydrolase fold. More experimental studies are required to expand the scope of two proposed strategies, such as, investigating the solvation phenomenon, examining the substitutions in other types of enzymes, or testing the additive effect by recombination. Our experimental studies on recombining the BSLA beneficial substitutions are in progress and will be reported in due course.

5. Computational and Experimental Section

5.1. Molecular dynamics simulations

The starting structure for all simulations was taken from crystal structure of BSLA wild type (PDB ID: 1I6 W,[25] Chain A, resolution 1.5 Å). The GROMOS96 (54a7) force field was used for the simulations of BSLA in DOX, DMSO, TFE. This force field has been reported to be a reliable force field for simulations of OSs and proteins.[35,63] The protonation state of ionizable residues was defined corresponding to pH 7.4. The histidine (His156), which is a part of the catalytic triad, was treated neutral with the proton on N_δ atom so that it could form the essential hydrogen bond (H-bond) with the negatively charged Asp133. The resulting system has a net charge of zero. Structures were solvated into a cubic box of SPCE water molecules[64] using periodic boundary. All organic solvent structures (DOX, DMSO, and TFE) were taken from ATB (Automated force field Topology Builder) with the parameter set of GROMOS96 (54a7) force field.[65] All organic solvent structures (DOX, DMSO, and TFE) were firstly taken from ATB (Automated force field Topology Builder) with the parameter set of GROMOS96 (54a7) force field.[65] Then the parameters of each model were modified according to the reported models.[66] In order to further validate OSs force field parameters, triplicate10 ns MD simulations were performed using both pure OS and OS-water mixtures to determine reproducibility of the experimental property (Table S7, see detailed procedures in SI). It was observed that OSs density obtained from MD simulations showed good agreement with experimental density of all three OSs. The OS systems were prepared according to experimental conditions, i.e., 22% (v/v) DOX, 60% (v/v) DMSO and 12% (v/v) TFE in water in a simulation box (volume: 500 nm^3). The box was filled with around 15764 water molecules in water only system, 531 DOX molecules and 12653 water molecules in DOX system, 1932 DMSO molecules, and 7475 water molecules in DMSO system, 507 TFE molecules and 13619 water molecules in TFE system, respectively.

In all cases, the system was carefully minimized and equilibrated using the following protocol. First, 1000 steps of energy minimization were carried for protein using steepest descent algorithm until it converged with a force tolerance of 500 $kJ\,mol^{-1}\,nm^{-1}$. Then,

5000 steps of energy minimization were carried only for solvent molecules with a force tolerance of 250 kJ mol^{-1}nm^{-1} after filling the box with water and OSs. After minimization, each system was equilibrated to 298 K through a stepwise heating protocol in the NVT ensemble followed by 100 ps equilibration in the NPT ensemble with position restraints on the protein molecule. The production simulation time for all systems was chosen to be 100 ns, in which RMSD achieved the stable conformation that providing reliable data for comparing with experimental studies. 298 K and 1 bar with using a time step of 1 fs were used for all systems after the protein relaxed. For each system, three independent MD simulation runs with different starting atomic velocities were run to avoid artifacts. Root mean square deviation (RMSD), radius of gyration (R_g), root mean square fluctuation per residue (RMSF), B-factor, solvent accessible surface area (SASA), H-bonds, second structure change (DSSP), radial distribution function (RDF), spatial distribution function (SDF), contact analysis were calculated by GROMACS tools. Pymol[67] and VMD 1.9.2[68] were used to analyze the structural change of protein, interactions between BSLA and OSs, salt bridges, and distance measurement. Molecular Mechanics-Poisson Boltzmann Surface Area (MM-PBSA) approach, which is an effective method for the calculation of biomolecular complexes,[69] was used to calculate the binding free energy as applied previously.[70] g_mmpbsa tools were applied with the default setting for the analysis of snapshots taken from MD trajectories of BSLA in OSs.[69a,71] The default solvent dielectric constant of 80 was taken,[69a] which is close to the real experimental dielectric constant of water and OS mixtures (Table S7). All molecular dynamics (MD) simulations were performed using GROMACS v5.1.2 software.[72] Furthermore, a detailed system setup for molecular docking is described in SI.

5.2. Analysis of "BSLA-SSM" library

Chemically competent *Escherichia coli* DH5a and *Escherichia coli* BL21-Gold (DE3) (Agilent Technologies; Santa Clara, USA) were used as hosts for plasmids amplification and protein expression, respectively. The plasmid pET22b(+)-bsla wild type was constructed in the previous work.[18f] A detailed description of the "BSLA-SSM" library generation and the activity assay with pNPB in 96-well MTP was reported in our previous studies.[18f] BSLA resistance (wild type or variant) was evaluated as activity in the presence of OSs divided by activity in the absence of OSs (see equations 1 and 2 in Supporting information (SI)). The concentration of OSs (22% (v/v) DOX, 60% (v/v) DMSO, and 12% (v/v) TFE) resulting in a residual BSLA activity of ~30% were chosen for the experiment because the concentration of each OS had proven as a good compromise between the reliable enzyme's activity and the enzyme's resistance compared to BSLA wild type in previous studies.[20–21] The beneficial substitution was defined as a substitution that increases BSLA resistance ($R_V \geq R_{WT} + 3\sigma$) to the respective OS.[17c] Properties of selected OSs were shown in Table S7. Furthermore, a detailed expression of BSLA in flask, purification, and characterization of purified BSLA wild type in OSs are described in SI.

Acknowledgments

Haiyang Cui is supported by a Ph.D. scholarship from the China Scholarship Council (CSC No. 201604910840). Simulations were performed with computing resources granted by JARA-HPC from RWTH Aachen University under projects JARA0169.

Conflict of Interest

The authors declare no conflict of interest.

Keywords: directed evolution · molecular dynamics simulation · biocatalysis · organic solvent · *Bacillus subtilis* Lipase A

[1] a) E. P. Hudson, R. K. Eppler, D. S. Clark, *Curr. Opin. Biotechnol.* **2005**, *16*, 637–643; b) K. M. Polizzi, A. S. Bommarius, J. M. Broering, J. F. Chaparro-Riggers, *Curr. Opin. Chem. Biol.* **2007**, *11*, 220–225; c) P. Kaul, Y. Asano, *Microb. Biotechnol.* **2012**, *5*, 18–33.
[2] a) M. N. Gupta, *Eur. J. Biochem.* **1992**, *203*, 25–32; b) A. M. Klibanov, *Nature* **2001**, *409*, 241; c) G. Carrea, S. Riva, *Angew. Chem. Int. Ed.* **2000**, *39*, 2226–2254; *Angew. Chem.* **2000**, *112*, 2312–2341.
[3] S. Dutta Banik, M. Nordblad, J. M. Woodley, G. H. Peters, *ACS Catal.* **2016**, *6*, 6350–6361.
[4] a) F. H. Arnold, *FASEB J.* **1993**, *7*, 744–749; b) G. R. Castro, T. Knubovets, *Crit. Rev. Biotechnol.* **2003**, *23*, 195–231; c) L. A. S. Gorman, J. S. Dordick, *Biotechnol. Bioeng.* **1992**, *39*, 392–397.
[5] a) S. Wang, X. Meng, H. Zhou, Y. Liu, F. Secundo, Y. Liu, *Catalysts* **2016**, *6*, 32; b) C. Lombard, J. Saulnier, J. Wallach, *Protein Pept. Lett.* **2005**, *12*, 621–629.
[6] a) N. Doukyu, H. Ogino, *Biochem. Eng. J.* **2010**, *48*, 270–282; b) A. Gupta, S. K. Khare, *Crit. Rev. Biotechnol.* **2009**, *29*, 44–54.
[7] a) J. Langlet, N. Gresh, C. Giessnerprettre, *Biopolymers* **1995**, *36*, 765–780; b) G. Colombo, G. Carrea, *J. Biotechnol.* **2002**, *96*, 23–33; c) G. Colombo, G. Ottolina, G. Carrea, *Monatsh. Chem.* **2000**, *131*, 527–547.
[8] V. Stepankova, S. Bidmanova, T. Koudelakova, Z. Prokop, R. Chaloupkova, J. Damborsky, *ACS Catal.* **2013**, *3*, 2823–2836.
[9] a) N. Yaacob, N. H. Ahmad Kamarudin, A. T. C. Leow, A. B. Salleh, R. N. Z. Raja Abd Rahman, M. S. Mohamad Ali, *Molecules* **2017**, *22*; b) K. Watanabe, T. Yoshida, S. Ueji, *Bioorg. Chem.* **2004**, *32*, 504–515.
[10] a) R. H. Valivety, P. J. Halling, A. D. Peilow, A. R. Macrae, *Biochim. Biophys. Acta Protein Struct. Mol. Enzymol.* **1992**, *1122*, 143–146; b) P. P. Wangikar, P. C. Michels, D. S. Clark, J. S. Dordick, *J. Am. Chem. Soc.* **1997**, *119*, 70–76; c) A. L. Serdakowski, J. S. Dordick, *Trends Biotechnol.* **2008**, *26*, 48–54; d) A. M. Klibanov, *Trends Biotechnol.* **1997**, *15*, 97–101; e) A. K. Chaudhary, S. V. Kamat, E. J. Beckman, D. Nurok, R. M. Kleyle, P. Hajdu, A. J. Russell, *J. Am. Chem. Soc.* **1996**, *118*, 12891–12901.
[11] a) M. Graber, R. Irague, E. Rosenfeld, S. Lamare, L. Franson, K. Hult, *Biochim. Biophys. Acta Protein Struct. Mol. Enzymol.* **2007**, *1774*, 1052–1057; b) R. H. Valivety, P. J. Halling, A. R. Macrae, *Biotechnol. Lett.* **1993**, *15*, 1133–1138; c) R. Bovara, G. Carrea, G. Ottolina, S. Riva, *Biotechnol. Lett.* **1993**, *15*, 937–942; d) M. L. Foresti, M. Galle, M. L. Ferreira, L. E. Briand, *J. Chem. Technol. Biotechnol.* **2009**, *84*, 1461–1473.
[12] a) A. S. Kim, L. T. Kakalis, N. Abdul-Manan, G. A. Liu, M. K. Rosen, *Nature* **2000**, *404*, 151–158; b) Z. Xu, R. Affleck, P. Wangikar, V. Suzawa, J. S. Dordick, D. S. Clark, *Biotechnol. Bioeng.* **1994**, *43*, 515–520.
[13] A. Ducret, M. Trani, R. Lortie, *Enzyme Microb. Technol.* **1998**, *22*, 212–216.
[14] R. Wedberg, J. Abildskov, G. H. Peters, *J. Phys. Chem. B* **2012**, *116*, 2575–2585.
[15] M. Z. Kamal, P. Yedavalli, M. V. Deshmukh, N. M. Rao, *Protein Sci.* **2013**, *22*, 904–915.
[16] U. T. Bornscheuer, B. Hauer, K. E. Jaeger, U. Schwaneberg, *Angew. Chem. Int. Ed.* **2019**, *58*, 36–40.
[17] a) H. J. Park, J. C. Joo, K. Park, Y. J. Yoo, *Biotechnol. Bioprocess Eng.* **2012**, *17*, 722–728; b) T. Kawata, H. Ogino, *Biotechnol. Prog.* **2009**, *25*, 1605–1611; c) U. Markel, L. Zhu, V. J. Frauenkron-Machedjou, J. Zhao, M. Bocola, M. D. Davari, K. E. Jaeger, U. Schwaneberg, *Catalysts* **2017**, *7*, 142; d) G. Careri, *Prog. Biophys. Mol. Biol.* **1998**, *70*, 223–249; e) A. Badoei-Dalfard, K. Khajeh, S. M. Asghari, B. Ranjbar, H. R. Karbalaei-Heidari, *J. Biochem.* **2010**, *148*, 231–238; f) H. Takagi, K. Hirai, Y. Maeda, H. Matsuzawa, S. Nakamori, *J. Biochem.* **2000**, *127*, 617–625; g) T. Koudelakova, R. Chaloupkova, J. Brezovsky, Z. Prokop, E. Sebestova, M. Hesseler, M. Khabiri, M. Plevaka, D. Kulik, I. Kuta Smatanova, P. Rezacova, R. Ettrich, U. T. Bornscheuer, J. Damborsky, *Angew. Chem. Int. Ed.* **2013**, *52*, 1959–1963; *Angew. Chem.* **2013**, *125*, 2013–2017.
[18] a) S. Bershtein, M. Segal, R. Bekerman, N. Tokuriki, D. S. Tawfik, *Nature* **2006**, *444*, 929–932; b) E. Firnberg, J. W. Labonte, J. J. Gray, M. Ostermeier, *Mol. Biol. Evol.* **2014**, *31*, 1581–1592; c) S. A. Funke, N. Otte,

T. Eggert, M. Bocola, K. E. Jaeger, W. Thiel, *Protein Eng. Des. Sel.* **2005**, *18*, 509–514; d) K. S. Sarkisyan, D. A. Bolotin, M. V. Meer, D. R. Usmanova, A. S. Mishin, G. V. Sharonov, D. N. Ivankov, N. G. Bozhanova, M. S. Baranov, O. Soylemez, *Nature* **2016**, *533*, 397–401; e) J. Y. van der Meer, H. Poddar, B. J. Baas, Y. Miao, M. Rahimi, A. Kunzendorf, R. van Merkerk, P. G. Tepper, E. M. Geertsema, A. M. W. Thunnissen, *Nat. Commun.* **2016**, *7*, 1–16; f) V. J. Frauenkron-Machedjou, A. Fulton, J. Zhao, L. Weber, K. E. Jaeger, U. Schwaneberg, L. Zhu, *Bioresour Bioprocess* **2018**, *5*, 2.

[19] S. Pramanik, G. V. Dhoke, K. E. Jaeger, U. Schwaneberg, M. D. Davari, *ACS Sustainable Chem. Eng.* **2019**, *7*, 11293–11302.

[20] V. J. Frauenkron-Machedjou, A. Fulton, L. Zhu, C. Anker, M. Bocola, K. E. Jaeger, U. Schwaneberg, *ChemBioChem* **2015**, *16*, 937–945.

[21] A. Fulton, V. J. Frauenkron-Machedjou, P. Skoczinski, S. Wilhelm, L. L. Zhu, U. Schwaneberg, K. E. Jaeger, *ChemBioChem* **2015**, *16*, 930–936.

[22] A. M. Duarte, C. P. van Mierlo, M. A. Hemminga, *J. Phys. Chem. B* **2008**, *112*, 8664–8671.

[23] a) Z. W. Yu, P. J. Quinn, *Biosci. Rep.* **1994**, *14*, 259–281; b) E. Moulin, V. Zoete, S. Barluenga, M. Karplus, N. Winssinger, *J. Am. Chem. Soc.* **2005**, *127*, 6999–7004; c) M. Svedendahl, P. Carlqvist, C. Branneby, O. Allnér, A. Frise, K. Hult, P. Berglund, T. Brinck, *ChemBioChem* **2008**, *9*, 2443–2451; d) J. L. Nieva, V. Madan, L. Carrasco, *Nat. Rev. Microbiol.* **2012**, *10*, 563–574.

[24] a) G. A. Jeffrey, *An introduction to hydrogen bonding, Vol. 32*, Oxford university press New York, **1997**; b) N. M. Micaêlo, C. M. Soares, *FASEB J.* **2007**, *274*, 2424–2436; c) M. J. Thiele, M. D. Davari, M. König, I. Hofmann, N. O. Junker, T. Mirzaei Garakani, L. Vojcic, J. Fitter, U. Schwaneberg, *ACS Catal.* **2018**, *8*, 10876–10887.

[25] G. van Pouderoyen, T. Eggert, K. E. Jaeger, B. W. Dijkstra, *J. Mol. Biol.* **2001**, *309*, 215–226.

[26] S. Shiraga, M. Ishiguro, H. Fukami, M. Nakao, M. Ueda, *Appl. Microbiol. Biotechnol.* **2005**, *68*, 779–785.

[27] K. P. Tan, T. B. Nguyen, S. Patel, R. Varadarajan, M. S. Madhusudhan, *Nucleic Acids Res.* **2013**, *41*, W314–W321.

[28] P. Lijnzaad, P. Argos, *Proteins Struct. Funct. Bioinf.* **1997**, *28*, 333–343.

[29] V. Kumar, P. Yedavalli, V. Gupta, N. M. Rao, *Protein Eng. Des. Sel.* **2014**, *27*, 73–82.

[30] N. Otte, M. Bocola, W. Thiel, *J. Comput. Chem.* **2009**, *30*, 154–162.

[31] T. Zisis, P. L. Freddolino, P. Turunen, M. C. Teeseling, A. E. Rowan, K. G. Blank, *Biochemistry* **2015**, *54*, 5969–5979.

[32] J. C. Hermann, E. Ghanem, Y. Li, F. M. Raushel, J. J. Irwin, B. K. Shoichet, *J. Am. Chem. Soc.* **2006**, *128*, 15882–15891.

[33] a) D. Chakravorty, S. Parameswaran, V. K. Dubey, S. Patra, *Appl. Biochem. Biotechnol.* **2012**, *167*, 439–461; b) M. T. Reetz, P. Soni, L. Fernandez, Y. Gumulya, J. D. Carballeira, *Chem. Commun. (Camb.)* **2010**, *46*, 8657–8658; c) H. Ogino, T. Uchiho, N. Doukyu, M. Yasuda, K. Ishimi, H. Ishikawa, *Biochem. Biophys. Res. Commun.* **2007**, *358*, 1028–1033.

[34] a) M. Zumárraga, F. J. Plou, H. García-Arellano, A. Ballesteros, M. Alcalde, *Biocatal. Biotransform.* **2007**, *25*, 219–228; b) S. Kumar, L. Sun, H. Liu, B. Muralidhara, J. R. Halpert, *Protein Eng. Des. Sel.* **2006**, *19*, 547–554.

[35] Z. Zou, H. Alibiglou, D. M. Mate, M. D. Davari, F. Jakob, U. Schwaneberg, *Chem. Commun. (Camb.)* **2018**, *54*, 11467–11470.

[36] M. Bellissent-Funel, A. Hassanali, M. Havenith, R. Henchman, P. Pohl, F. Sterpone, D. Spoel, Y. Xu, A. E. Garcia, *Chem. Rev.* **2016**, *116*, 7673–7697.

[37] J. N. Dahanayake, K. R. Mitchell-Koch, *Front. Mol. Biosci.* **2018**, *5*, 65.

[38] G. Bell, A. E. Janssen, P. J. Halling, *Enzyme Microb. Technol.* **1997**, *20*, 471–477.

[39] J. i Vyměťal, L. Bednárová, J. i Vondrášek, *J. Phys. Chem. B* **2016**, *120*, 1048–1059.

[40] A. Kumar, K. Dhar, S. S. Kanwar, P. K. Arora, *Biol. Proced. Online* **2016**, *18*, 2.

[41] C. H. Wong, S. T. Chen, W. J. Hennen, J. A. Bibbs, Y. Wang, J. L. Liu, M. W. Pantoliano, M. Whitlow, P. N. Bryan, *J. Am. Chem. Soc.* **1990**, *112*, 945–953.

[42] X. Li, H. Y. Yu, *J. Ind. Microbiol. Biotechnol.* **2012**, *39*, 1117–1124.

[43] a) D. Roccatano, T. S. Wong, U. Schwaneberg, M. Zacharias, *Biopolymers* **2006**, *83*, 467–476; b) D. Lousa, A. M. Baptista, C. M. Soares, *Phys. Chem. Chem. Phys.* **2013**, *15*, 13723–13736.

[44] B. A. Tejo, A. B. Salleh, J. Pleiss, *J. Mol. Model.* **2004**, *10*, 358–366.

[45] a) J. T. King, E. J. Arthur, C. L. Brooks III, K. J. Kubarych, *J. Phys. Chem. B* **2012**, *116*, 5604–5611; b) Y. Qin, L. Wang, D. Zhong, *Proc. Natl. Acad. Sci. USA* **2016**, *113*, 8424–8429; c) T. Oroguchi, M. Nakasako, *Sci. Rep.* **2016**, *6*, 26302; d) S. Ebbinghaus, S. J. Kim, M. Heyden, X. Yu, U. Heugen, M. Gruebele, D. M. Leitner, M. Havenith, *Proc. Natl. Acad. Sci. USA* **2007**, *104*, 20749–20752.

[46] C. Li, T. Tan, H. Zhang, W. Feng, *J. Biol. Chem.* **2010**, *285*, 28434–28441.

[47] a) A. M. Slovic, H. Kono, J. D. Lear, J. G. Saven, W. F. DeGrado, *Proc. Natl. Acad. Sci. USA* **2004**, *101*, 1828–1833; b) S. R. Trevino, J. M. Scholtz, C. N. Pace, *J. Mol. Biol.* **2007**, *366*, 449–460; c) K. W. Pulsipher, J. A. Villegas, B. W. Roose, T. L. Hicks, J. Yoon, J. G. Saven, I. J. Dmochowski, *Biochemistry* **2017**, *56*, 3596–3606.

[48] S. Park, X. Yang, J. G. Saven, *Curr. Opin. Struct. Biol.* **2004**, *14*, 487–494.

[49] C. A. Schramm, B. T. Hannigan, J. E. Donald, C. Keasar, J. G. Saven, W. F. DeGrado, I. Samish, *Structure* **2012**, *20*, 924–935.

[50] P. Sears, M. Schuster, P. Wang, K. Witte, C. H. Wong, *J. Am. Chem. Soc.* **1994**, *116*, 6521–6530.

[51] P. R. Burney, E. M. Nordwald, K. Hickman, J. L. Kaar, J. Pfaendtner, *Proteins Struct. Funct. Bioinf.* **2015**, *83*, 670–680.

[52] a) A. J. Russell, A. R. Fersht, *Nature* **1987**, *328*, 496; b) A. J. Russell, P. G. Thomas, A. R. Fersht, *J. Mol. Biol.* **1987**, *193*, 803–813.

[53] D. A. Estell, T. P. Graycar, J. A. Wells, *J. Biol. Chem.* **1985**, *260*, 6518–6521.

[54] J. Zhao, V. J. Frauenkron-Machedjou, A. Fulton, L. Zhu, M. D. Davari, K. E. Jaeger, U. Schwaneberg, M. Bocola, *Phys. Chem. Chem. Phys.* **2018**, *20*, 9600–9609.

[55] a) M. T. Reetz, M. Bocola, J. D. Carballeira, D. Zha, A. Vogel, *Angew. Chem. Int. Ed.* **2005**, *117*, 4264–4268; b) M. T. Reetz, L. W. Wang, M. Bocola, *Angew. Chem. Int. Ed.* **2006**, *45*, 1236–1241; *Angew. Chem.* **2006**, *118*, 1258–1263.

[56] H. Cui, H. Cao, H. Cai, J. Karl-Erich, M. D. Davari, U. Schwaneberg, *Chem. Eur. J.* **2020**, *26*, 643–649.

[57] Z. Sun, R. Lonsdale, X. Kong, J. Xu, J. Zhou, M. T. Reetz, *Angew. Chem. Int. Ed.* **2015**, *54*, 12410–12415; *Angew. Chem.* **2015**, *127*, 12587–12592.

[58] K. Liebeton, A. Zonta, K. Schimossek, M. Nardini, D. Lang, B. W. Dijkstra, M. T. Reetz, K. E. Jaeger, *Cell Chem. Biol.* **2000**, *7*, 709–718.

[59] M. T. Reetz, J. D. Carballeira, *Nat. Protoc.* **2007**, *2*, 891.

[60] A. Dennig, A. V. Shivange, J. Marienhagen, U. Schwaneberg, *PLoS One* **2011**, *6*, e26222.

[61] J. Marienhagen, A. Dennig, U. Schwaneberg, *BioTechniques* **2012**, *52*.

[62] H. Zhao, W. Zha, *Nat. Protoc.* **2006**, *1*, 1865–1871.

[63] a) J. N. Dahanayake, D. N. Gautam, R. Verma, K. R. Mitchell-Koch, *Mol. Simul.* **2016**, *42*, 1001–1013; b) L. Migliolo, O. N. Silva, P. A. Silva, M. P. Costa, C. R. Costa, D. O. Nolasco, J. A. Barbosa, M. R. Silva, M. P. Bemquerer, L. M. Lima, *PLoS One* **2012**, *7*, e47047; c) Y. Jewel, T. Liu, A. Eyler, W. Zhong, J. Liu, *J. Phys. Chem. C* **2015**, *119*, 26760–26767; d) N. Schmid, A. P. Eichenberger, A. Choutko, S. Riniker, M. Winger, A. E. Mark, W. F. van Gunsteren, *Eur. Biophys. J.* **2011**, *40*, 843.

[64] P. Mark, L. Nilsson, *J. Phys. Chem. A* **2001**, *105*, 9954–9960.

[65] A. K. Malde, L. Zuo, M. Breeze, M. Stroet, D. Poger, P. C. Nair, C. Oostenbrink, A. E. Mark, *J. Chem. Theory Comput.* **2011**, *7*, 4026–4037.

[66] a) M. Fioroni, K. Burger, A. E. Mark, D. Roccatano, *J. Phys. Chem. B* **2000**, *104*, 12347–12354; b) D. P. Geerke, C. Oostenbrink, N. F. van der Vegt, W. F. van Gunsteren, *J. Phys. Chem. B* **2004**, *108*, 1436–1445; c) P. I. Nagy, G. Völgyi, K. Takács-Novák, *J. Phys. Chem. B* **2008**, *112*, 2085–2094; d) M. Taha, I. Khoiroh, M.-J. Lee, *J. Phys. Chem. B* **2013**, *117*, 563–582.

[67] W. L. DeLano, *http://www.pymol.org* **2002**.

[68] W. Humphrey, A. Dalke, K. Schulten, *J. Mol. Graphics* **1996**, *14*, 33–38.

[69] a) R. Kumari, R. Kumar, A. Lynn, *J. Chem. Inf. Model.* **2014**, *54*, 1951–1962; b) B. Gao, S. Jiang, L. Wang, L. Zhang, D. Wei, *Biochem. Eng. J.* **2018**, *129*, 106–112.

[70] a) M. Fu, L. Chen, L. Zhang, X. Yu, Q. Yang, *Int. J. Mol. Med.* **2017**, *39*, 1164–1172; b) B. K. Mai, M. S. Li, *Biochem. Biophys. Res. Commun.* **2011**, *410*, 688–691; c) J. Kumar, T. Umar, T. Kausar, M. Mobashir, S. M. Nayeem, N. Hoda, *J. Mol. Model.* **2017**, *23*, 7; d) S. Verma, S. Grover, C. Tyagi, S. Goyal, S. Jamal, A. Singh, A. Grover, *PLoS One* **2016**, *11*, e0149014.

[71] a) A. Weis, K. Katebzadeh, P. Söderhjelm, I. Nilsson, U. Ryde, *J. Med. Chem.* **2006**, *49*, 6596–6606; b) H. Sun, L. Duan, F. Chen, H. Liu, Z. Wang, P. Pan, F. Zhu, J. Z. Zhang, T. Hou, *Phys. Chem. Chem. Phys.* **2018**, *20*, 14450–14460.

[72] M. J. Abraham, T. Murtola, R. Schulz, S. Páll, J. C. Smith, B. Hess, E. Lindahl, *SoftwareX* **2015**, *1*, 19–25.

Manuscript received: March 10, 2020
Revised manuscript received: April 27, 2020
Accepted manuscript online: April 28, 2020
Version of record online: June 18, 2020